Continuum random sequential adsorption of polymer on a flat and homogeneous surface

Michał Cieśla*
M. Smoluchowski Institute of Physics, Jagiellonian University, 30-059 Krakow, Reymonta 4, Poland
(Received 30 January 2013; published 8 May 2013)

Random sequential adsorption (RSA) of polymer, modeled as a chain of identical spheres, is systematically studied. In order to control precisely anisotropy and number of degrees of freedom, two different kinds of polymers are used. In the first one, monomers are placed along a straight line, whereas in the second, relative orientations of particles are random. Such polymers fill a flat homogeneous surface randomly. The paper focuses on maximal random coverage ratio and adsorption kinetics dependence on polymer size, shape anisotropy, and numbers of degrees of freedom. Obtained results were discussed and compared with other numerical experiments and theoretical predictions.

DOI: 10.1103/PhysRevE.87.052401 PACS number(s): 68.43.Fg, 05.45.Df

I. INTRODUCTION

Irreversible adsorption of complex particles at solid and liquid interfaces is of major significance for many fields such as medicine and material sciences as well as pharmaceutical and cosmetic industries. For example, adsorption of some proteins plays crucial role in blood coagulation, inflammatory response, fouling of contact lenses, plaque formation, ultrafiltration, and membrane filtration units operation. Additionally, controlled adsorption is fundamental for efficient chromatographic separation and purification, gel electrophoresis, filtration, as well as performance of bioreactors, biosensing, and immunological assays.

Since its introduction by Feder [1], random sequential adsorption (RSA) became a well-established method of adsorption properties modeling, especially for spherical molecules. On the other hand, using RSA to simulate adsorption of more complicated particles, such as polymers or proteins, raises a question how the universal properties of RSA changes when it is applied to nonspherical molecules. The question has already been answered for basic shapes, e.g., spheroids, spherocylinders, rectangles, needles, and similar [2–6]. However, recent studies show that such shapes are not sufficient for modeling adsorption of common proteins, such as, for example, fibrinogen [7]. Therefore, attention of investigators has lately been drawn to coarse-grained modeling of complex biomolecules and polymers [8–12].

This study focuses on RSA of polymers on flat and homogeneous two-dimensional collector surface. A similar model has been investigated by Adamczyk *et al.* [13]; the authors, however, have studied adsorption on squared grid. Other works in this field used different polymers models, e.g., Ref. [14], or assumed specific conformations of polymers and used different simulation methods [15]. In all of them, authors have focused on proper modeling of a specific polymer and, therefore, numerical method used for adsorption modeling was treated only as a tool. Here, the main focus is set on properties of the tool. The main purpose of this work is to find out how the kinetics of RSA as well as basic characteristics of obtained adsorption monolayers depend on particle elongation and its number of degrees of freedom when the particle shape is approximated using coarse-grained approach. In our study, polymer is treated as a kind of a toy-model of complex molecules, where both shape anisotropy and number of degrees of freedom are easy to control by merely changing the number of monomers. Therefore, the model seems to be the simplest, yet universal tool for determining properties of RSA as well as complex particles adsorption.

II. MODEL

Polymer is modeled as a chain of identical, spherical monomers. In this study, two kinds of polymer models are used:

(i) stiff—monomers are placed along a straight line. In this model, elongation is controlled by number of monomers, whereas number of degrees of freedom remains constant;

(ii) flexible—monomer can rotate freely around its neighbors; however, it cannot overlap with other monomers. It is assumed that all monomers lay in a single plane. The number of degrees of freedom increases with monomer count, but the increase is nonlinear, due to excluded volume effect.

Maximal random coverages are generated using RSA algorithm, which is based on independent, repeated attempts of adding polymer to a covering layer. The numerical procedure is carried out in the following steps:

(i) a virtual polymer is randomly created in such way that the center of each monomer is located on a collector;

(ii) an overlapping test is performed for previously adsorbed nearest neighbors of the virtual polymer. The test checks if surface-to-surface distance between monomers is not less than zero;

(iii) If there is no overlap, the virtual polymer is irreversibly adsorbed and added to an existing covering layer. Its position does not change during further calculations;

(iv) if there is an overlap, the virtual polymer is removed and abandoned.

Attempts are repeated iteratively. Their number is commonly expressed in dimensionless time units:

$$t_0 = N\frac{S_P}{S_C}, \tag{1}$$

where N is a number of attempts, S_P denotes surface area of a single polymer projection on a collector, and S_C is the collector area. Here, $S_P = n\pi r_0^2$ for polymers built of n spherical

*michal.ciesla@uj.edu.pl

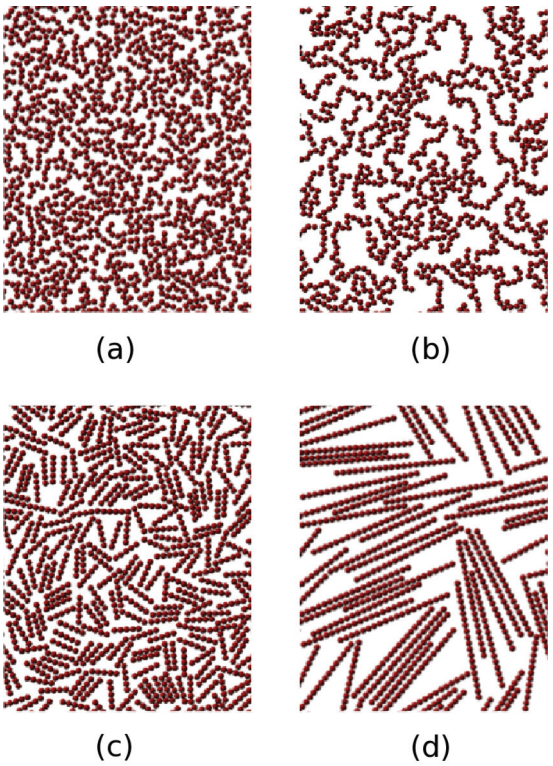

FIG. 1. (Color online) Fragments of example layers formed after $t_0 = 10^5$ by flexible (a), (b) and stiff (c), (d) polymer RSA. The polymers are made of 5 monomers (a), (c) and 20 monomers (b), (d). Coverage ratios are: (a) −0.489, (b) −0.356, (c) −0.464, and (d) −0.345.

monomers of radius r_0. Square surface of $S_C = (400r_0)^2$, with no boundary conditions. Although, in general, specific boundary conditions can influence on obtained results, it has been proved that in the case of dimer ($n = 2$), there is no such effect for large enough collectors [16]. The total number of iterations in each simulation was $10^5 t_0$. Analyzed polymers were built of 2 to 20 monomers. For each polymer size and type, 100 independent numerical experiments have been performed.

III. RESULTS AND DISCUSSION

Example layers obtained from numerical simulations described in Sec. II are presented in Fig. 1. The main parameter characterizing obtained layers is coverage ratio:

$$\theta(t) = n_P(t)\frac{S_P}{S_C}, \tag{2}$$

which, after infinite iteration of RSA algorithm, approaches the maximal random coverage ratio $\theta_{\max} = \theta(t \to \infty)$. Parameter n_P denotes here number of adsorbed polymers. To effectively measure $\theta_{\max}$ using finite-time computer simulations, appropriate model of adsorption kinetics is needed.

A. RSA kinetics

Adsorption kinetics can be described analytically for two cases: low coverage limit and jamming limit [5,6]. In general, probability of adsorption depends on uncovered collector area described by available surface function (ASF). For example, when coverage is very low, ASF decreases linearly with a number of adsorbed particles. When coverage increases, the ASF decay slows down as two or more particles can block the same space; e.g., see Ref. [17]. Therefore, for a low coverage limit, the ASF is often approximated by

$$B(\theta) = 1 - C_1\theta + C_2\theta^2 + o(\theta^2), \tag{3}$$

where C_1 corresponds to an area blocked by single molecule and C_2 accounts overlapping of those areas [17]. It is worth noting that C_1 and C_2 are directly connected with viral coefficients, which can be also calculated from Meyers diagrams, describing adsorbate particles in thermodynamic equilibrium. In the case of stiff polymer, the particle shape can be approximated by a spherocylinder. Then, $C_{1\,(\mathrm{SC})}$ can be analytically derived as [18]

$$C_{1\,(\mathrm{SC})} = 2\left(1 + \frac{L^2}{4\pi A}\right) = 2\left\{1 + \frac{[2\pi + 4(n-1)]^2}{4\pi[\pi + 4(n-1)]}\right\}, \tag{4}$$

where L is convex particle perimeter and A is its area. Though spherocylinder approximates surface blocked by adsorbed polymer particle properly, its area is slightly larger than the polymer model area. Therefore, $C_{1\,(\mathrm{SC})}$ underestimates the real value and should be multiplied by a ratio of those areas:

$$C_1 = C_{1\,(\mathrm{SC})}\frac{\pi + 4(n-1)}{n\pi} \approx \frac{8}{\pi}\left(1 + \frac{n}{\pi}\right), \quad \text{for large } n. \tag{5}$$

Parameter C_2 can be obtained only numerically; e.g., see Ref. [19]. In the case of the flexible chain, there are no analytical predictions for either C_1 or C_2 when $n > 1$.

Parameter C_1 has been numerically estimated by fitting $B(\theta)$ defined as Eq. (3) for $\theta \leqslant 0.2\theta_{\max}$. For stiff polymer, values obtained comply well with the predicted Eq. (5). For flexible polymer, C_1 grows with the number of monomers, which can be approximated with a power law (see Fig. 2). As expected, stiff polymer particle blocks more area than the flexible one. Moreover, C_1 growth with polymer size is significantly faster for a linear particle.

The second limit of RSA kinetics (collector almost maximally filled) is of major importance for determining maximal random coverage ratio based on finite-time simulations.

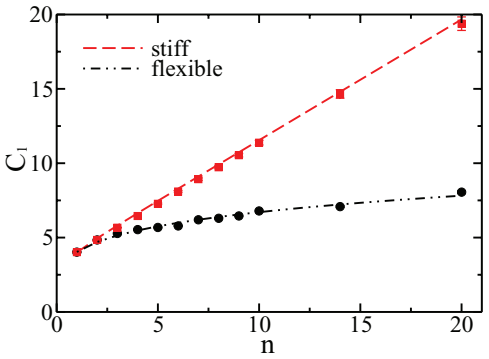

FIG. 2. (Color online) Dependence of blocking parameter C_1 on polymer size. Dots and squares are simulation data for flexible and stiff polymer, respectively, whereas lines corresponds to fits: Eq. (5) for stiff polymer and $C_1 = 4.03\,n^{0.22}$ for the flexible one.

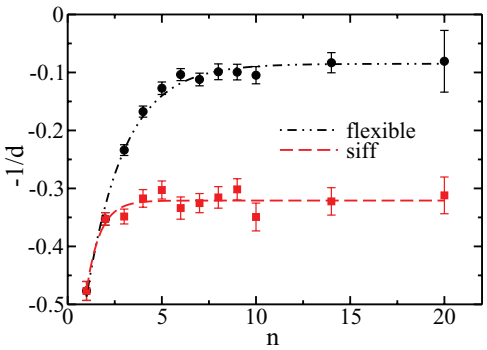

FIG. 3. (Color online) Dependence of exponent in Eq. (6) on polymer size. Dots and squares are simulation data, whereas lines correspond to exponential fits: $(-0.32 - 0.54\exp[-1.28\,n])$ for stiff polymer and $(-0.09 - 0.65\exp[-0.49\,n])$ for the flexible one.

Coverage growth is then governed by Feder's law [1,20–22]:

$$\theta(t) = \theta_{\max} - A\,t^{-\frac{1}{d}}, \tag{6}$$

where A is a coefficient and d is interpreted as collector dimension [20] in the case of spherical particles adsorption or more generally as a number of degrees of freedom [22]. Feder's law was confirmed for RSA of spheres in several collector dimensions [23], including nonintegral [24,27], as well as for elongated particles [6,25]. The analysis of exponent in Eq. (6) estimated using coverage ratio growth presented in Fig. 3 reveals at least three things worth noting. First, the value for $n = 1$ (spheres) is close to -0.5 as predicted theoretically [20] and confirmed in earlier studies; e.g., see Refs. [1,23]. Second, the value for the dimer case ($n = 2$) is significantly higher, which reflects more degrees of freedom for such particles. This result differs from one obtained earlier [16]. It results from a less accurate approximation method used there. Third, the stiff polymer exponent approaches $d \approx 3$ for $n \geqslant 3$, which reflects third, orientational degree of freedom, and stays at this level despite further increase in monomers number. In the case of flexible polymer, the increase is also curbed, but at higher $d \approx 10$ value. It suggest that hard-core interaction between monomers limits an infinite growth of the number of degrees of freedom with polymer length.

B. Maximal random coverage ratio

The maximal random coverage ratios were determined by extending obtained RSA kinetics to infinite time. Note that according to the Eq. (6), the set of points $[t^{-1/d},\theta(t)]$ obtained from the numerical simulations will form a straight line. By approximating this line up to $t^{-1/d} = 0$, one can find $\theta_{\max}$. Note that the prior knowledge of exponent $-1/d$ estimated in Sec. III A is essential to get proper values of the maximal random coverage ratio. Results obtained in this way are presented in Fig. 4. The analysis of RSA of dimer shows, within error margin, the same maximal random coverage ratio for spheres as obtained for dimers [16]. This almost constant value of the ratio is observed in the range of $n \leqslant 6$, but only for flexible polymer model. Then, rapid decay of coverage ratio is observed. The existence of the plateau is unexpected. Similar study of RSA on a square lattice shows that the maximal random coverage ratio decreases exponentially with a polymer

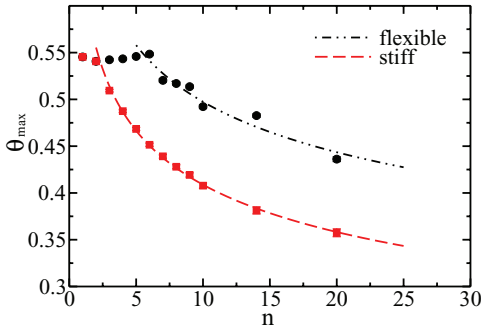

FIG. 4. (Color online) Dependence of maximal random coverage ratio on polymer size. Dots and squares are simulation data, whereas lines correspond to power fits: $0.63\,n^{-0.19}$ for stiff polymer and $0.73\,n^{-0.17}$ for the flexible one.

size [28]. However, here on a continuous surface there are at least two competing factors affecting the maximal random coverage ratio. The first is similar to the lattice case—larger particles are harder to place on a collector due to lower probability of finding a large enough uncovered space. The second factor is a higher packing ratio of monomers in a polymer globule than in a set of independent monomers. The second factor is more important for continuous collectors than for lattice ones, due to larger possibility of forming a globule when it is needed. Therefore, in the case of flexible polymer adsorption, competitions of those two factors results in almost constant coverage ratio up to $n \leqslant 6$. There is no such effect for stiff polymer, because there the second factor counts only for $n = 2$. The same reason explains much lower (approx. 20%) values of the maximal random coverage ratio obtained for stiff polymer adsorption. In both the cases, the decay of $\theta_{\max}$ for large enough polymer length can be approximated by a power or exponential function. To fully discriminate between these two types of relationship, the range of studied polymer lengths should be significantly extended.

C. Density autocorrelation and orientational ordering

Density autocorrelation function $G(r)$, also known as two-point correlation function, is defined here as a mean probability of finding two monomers at distance r, regardless of whether they come from the same polymer chain or from different particles. Because the density autocorrelation function depends on the coverage ratio, which is in general different for different polymer length and model, here we decide to calculate density for the coverage ratio close to the maximal one but equal for all presented cases. Such plot of the $G(r)$ is presented in Fig. 5. In case of spheres, the density autocorrelation function for maximal random coverages exhibits some universal properties, such as logarithmic singularity for $r \to 2r_0^+$ [20,21] and fast superexponential decay when $r \gg r_0$ [26]. However, even for relatively short polymers, those properties cannot be observed, due to periodic structure of particles (especially in a stiff polymer). On the other hand, at distances larger than polymer length, almost no density correlation is observed.

Elongated particle can form orientationally ordered structures, e.g., liquid crystals. For RSA on infinite collector, when particles orientations are randomly selected according to uniform probability distribution, there is no reason for the

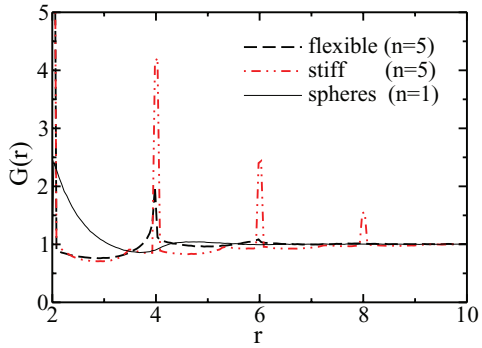

FIG. 5. (Color online) Density autocorrelation function. Data for $n = 5$ for flexible and stiff polymers were plotted together with data for spheres ($n = 1$) used here as a reference level. All functions were obtained for the same coverage ratio $\theta = 0.461$ and were normalized to a mean density of monomers and, therefore, they oscillate around $G(r) = 1$.

global orientational order to appear. Nevertheless, forming of local ordered domains is possible [16,27] because parallely aligned particles require less space (see also Fig. 1). Therefore, subsequent adsorbed polymers will align parallel to their neighbors, especially when adsorption approaches jamming limit. Situation changes when adsorption on finite collectors is investigated. Adsorption conditions at collector boundaries may promote specific ordering. To measure it quantitatively, the order parameter has to be defined [25].

$$q = 2\left[\frac{1}{N}\sum_{i=1}^{N}(x_i\cos\phi + y_i\sin\phi)^2 - \frac{1}{2}\right], \qquad (7)$$

where N is a number of molecules in a layer, $[x_i, y_i]$ is a unit vector pointing from one end of the polymer to the other, and ϕ denotes mean direction of all particles and can be calculated as in Ref. [16]. Order parameter q is normalized so as to vanish in totally disordered layers and to equal 1 for perfectly ordered systems. The mean values of q for obtained coverages are presented in Fig. 6. As expected, global orientational order increases with polymer size; however, its value is rather small, even for the longest stiff polymer because collector area is relatively large.

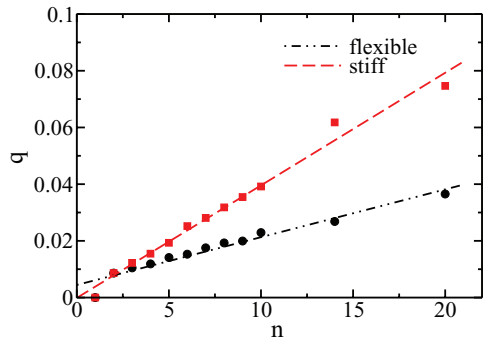

FIG. 6. (Color online) Dependence of global orientational order parameter on polymer size. Dots and squares are numerical data, whereas lines are linear fits: $-0.00013 + 0.0040n$ for stiff polymer and $y = 0.0044 + 0.0017n$ for flexible one.

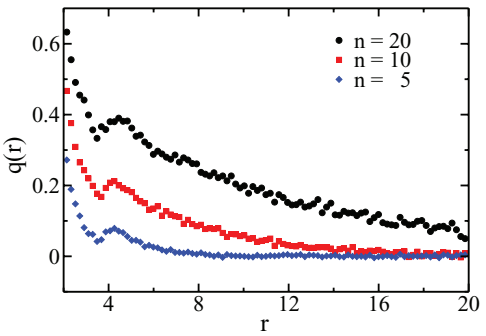

FIG. 7. (Color online) Local orientational ordering propagation inside covering layer built of stiff polymers.

To study local ordering, the following function was introduced:

$$q(|\vec{r}|) = 2\left[\langle[\phi(\vec{x})\cdot\phi(\vec{x}+\vec{r})]^2\rangle - \tfrac{1}{2}\right], \qquad (8)$$

where $\phi(\vec{x})$ is a unit vector along local orientational ordering at point $\vec{x}$ and $\langle\cdot\rangle$ is an average over particle pairs at a distance r, measured as a distance between centers of the closest monomers. Relation $q(r)$ shows how the local ordering propagates in a layer. As shown in Fig. 7, ordering vanishes quickly for short stiff polymers. For the longest one, it is significantly larger than 0 even at distance of $10r_0$, which reflects a tendency for parallel alignment. Slight minimum around $r_0 \approx 3.5$ is connected with the definition of distance between particles, which allows two, even perpendicular polymers, to be as close as parallel ones.

IV. SUMMARY

In the study, coarse-grain model of polymer is used to test dependence of RSA properties on number of degrees of freedom and elongation of adsorbate particles. RSA kinetics at low coverage limit is sensitive to molecule shape anisotropy, whereas at jamming limit it is governed by number of degrees of freedom, which generally is consistent with Feder's law predictions. Maximal random coverage ratios did not change for short ($n \leqslant 6$) flexible polymers, while rapid drop was observed for stiff polymer starting at $n = 3$. Density autocorrelations for maximally covered layers reflect the inner structure of adsorbate particles, especially for stiff polymers. Additionally, in that case, significant local orientational ordering was observed, which reflects domain structure of such layer.

Flexible and stiff polymer models discussed here are only two extreme possible cases. In fact, polymer stiffness is controlled by intramolecular interactions, which typically depend on environmental conditions. It is possible to extend the presented model of polymer by such interactions and find dependence of properties discussed here on, for example, temperature, in a way as in Refs. [29,30], where a similar RSA problem on a square and triangular lattice has been studied.

ACKNOWLDGMENT

This work was supported by Grant No. MNiSW/N N204 439040.

[1] J. Feder, J. Theor. Biol. **87**, 237 (1980).
[2] J. Talbot, G. Tarjus, and P. Schaaf, Phys. Rev. A **40**, 4808 (1989).
[3] R. D. Vigil and R. M. Ziff, J. Chem. Phys. **91**, 2599 (1989).
[4] G. Tarjus and P. Viot, Phys. Rev. Lett. **67**, 1875 (1991).
[5] P. Viot, G. Tarjus, S. M. Ricci, and J. Talbot, J. Chem. Phys. **97**, 5212 (1992).
[6] S. M. Ricci, J. Talbot, G. Tarjus, and P. Viot, J. Chem. Phys. **97**, 5219 (1992).
[7] Z. Adamczyk, J. Barbasz, and M. Ciesla, Langmuir **26**, 11934 (2010).
[8] Z. Adamczyk, J. Barbasz, and M. Ciesla, Langmuir **27**, 6868 (2011).
[9] M. Rabe, D. Verdes, and S. Seeger, Adv. Colloid Interface Sci. **162**, 87 (2011).
[10] C. Finch, T. Clarke, and J. J. Hickman, J. Comput. Phys. (2012), doi: 10.1016/j.jcp.2012.07.034.
[11] P. Katira, A. Agarwal, and H. Hess, Adv. Mater. **21**, 1599 (2012).
[12] Z. Adamczyk, Curr. Opin. Colloid Interface Sci. **17**, 173 (2012).
[13] P. Adamczyk, P. Romiszowski, and A. Sikorski, J. Chem. Phys. **128**, 154911 (2008).
[14] L.-C. Jia and P.-Y. Lai, J. Chem. Phys. **105**, 11319 (1996).
[15] A. Sikorski, Macromol. Theory Simul. **10**, 38 (2001).
[16] M. Ciesla and J. Barbasz, J. Stat. Mech. (2012) P03015.
[17] Z. Adamczyk, *Particles at Interfaces: Interactions, Deposition, Structure* (Elsevier/Academic Press, Amsterdam, 2006).
[18] T. Boublik, Mol. Phys. **29**, 421 (1975).
[19] Y. Martinez-Raton, E. Velasco, and L. Mederos, J. Chem. Phys. **125**, 014501 (2006).
[20] R. H. Swendsen, Phys. Rev. A **24**, 504 (1981).
[21] V. Privman, J.-S. Wang, and P. Nielaba, Phys. Rev. B **43**, 3366 (1991).
[22] E. L. Hinrichsen, J. Feder, and T. Jossang, J. Stat. Phys. **44**, 793 (1986).
[23] S. Torquato, O. U. Uche, and F. H. Stillinger, Phys. Rev. E **74**, 061308 (2006).
[24] M. Ciesla and J. Barbasz, J. Chem. Phys. **137**, 044706 (2012).
[25] M. Cieśla and J. Barbasz, Colloids Surf. B: Biointerfaces (2013), doi: 10.1016/j.colsurfb.2013.04.013.
[26] B. Bonnier, D. Boyer, and P. Viot, J. Phys. A **27**, 3671 (1994).
[27] J. Barbasz and M. Ciesla, arXiv:1301.4697 [cond-mat.mtrl-sci] (2013).
[28] Lj. Budinski-Petković and U. Kozmidis-Luburic, Physica A **236**, 211 (1997).
[29] G. Kondrat, J. Chem. Phys. **117**, 6662 (2002).
[30] G. Kondrat, Phys. Rev. E **78**, 011101 (2008).